This is a preprint of the paper:

Daniel Lerch-Hostalot, David Megías, *"Detection of Classifier Inconsistencies in Image Steganalysis"*, Proceedings of the ACM Workshop on Information Hiding and Multimedia Security, July 2019, Pages 222-229. ISBN: 978-1-4503-6821-6. https://doi.org/10.1145/3335203.3335738.

Detection of Classifier Inconsistencies in Image Steganalysis

Daniel Lerch-Hostalot
David Megías
Internet Interdisciplinary Institute (IN3), Universitat Oberta de Catalunya (UOC),
CYBERCAT-Center for Cybersecurity Research of Catalonia
Castelldefels, Barcelona, Spain
{dlerch,dmegias}@uoc.edu

ABSTRACT

In this paper, a methodology to detect inconsistencies in classification-based image steganalysis is presented. The proposed approach uses two classifiers: the usual one, trained with a set formed by *cover* and *stego* images, and a second classifier trained with the set obtained after embedding additional random messages into the original training set. When the decisions of these two classifiers are not consistent, we know that the prediction is not reliable. The number of inconsistencies in the predictions of a testing set may indicate that the classifier is not performing correctly in the testing scenario. This occurs, for example, in case of cover source mismatch, or when we are trying to detect a steganographic method that the classifier is no capable of modelling accurately. We also show how the number of inconsistencies can be used to predict the reliability of the classifier (classification errors).

KEYWORDS

Steganalysis, Cover Source Mismatch, Machine Learning

1 INTRODUCTION

Steganography is a collection of techniques to embed secret data into apparently innocent objects. Nowadays, these objects are mainly digital media, and the most common carriers for steganography are digital images because of their widespread use. On the other hand, steganalysis refers to different techniques used to detect messages previously hidden using steganography.

Most steganalytic methods in the state of the art use *machine learning* [3, 6, 7]. In machine learning-based steganalysis, firstly, a (training) set of known cover and stego images is used to train a classifier. Later on, this classifier is used to predict the images of a testing set as cover or stego.

This approach works very well in laboratory conditions, that is, if the set of training images is similar to that of the testing images used by the steganographer to hide secret data. However, in the real world, the set of media used by the steganographer might be quite different from that used to train the classifier [12]. This occurs, for example, when the images in the testing set are not well represented in the training set. Some examples of this mismatch occur if the testing images are taken using a different camera or resolution; if they are compressed, zoomed or improved through filters; or if they were taken in very different conditions. In steganalysis, this problem is known as *cover source mismatch* (CSM) and was initially reported in [4]. There are other situations that lead to inaccurate predictions. For example, *stego source mismatch* (SSM) occurs when some embedding parameter, such as the exact payload [20], differ between the training and the testing datasets.

Different approaches to the CSM problem have been proposed. During the BOSS competition [1], some participants tried an approach called "training on a contaminated database", which consists in denoising images from the testing set and including them in the training set [8]. A different approach is to make the training set as complete as possible. In [18], the authors trained a classifier with a huge variety of images. Due to the high time and memory requirements, this was carried out using on-line classifiers. In [14], three different strategies are presented: (1) training with a mixture of cover sources; (2) using different classifiers trained with different sources and testing with the closest source; and (3) taking the second approach but testing each image separately using the closest source. The *islet approach* [19], introduces a pre-processing step consisting in organizing the images in clusters and assigning a steganalyzer to each cluster. In [23], a scheme to efficiently construct a large and representative training set is proposed. Finally, in [16], an unsupervised steganalytic method was proposed that does not require a training set, bypassing the CSM problem.

In supervised machine learning-based steganalysis, we need a database of images to construct the training set and a validation set to determine the classification accuracy results. The creation of this database is a fundamental part of the process. Usually, this is carried out by collecting pictures taken with different cameras and models, taken in different lighting conditions, compressed with different algorithms and compressing ratios, processed with different filters, modified by optical or digital zoom, etc. If we create a database with pictures taken by a team of people with their cameras and with a specific set of filters, zooms, compression algorithms and so on, this will be a biased procedure, and such a selection can never represent the entire population of possible images. Even if we decide to download random images from the Internet, the combination of cameras, models, filters, compression ratios, light conditions, and so on, is too large and it is almost impossible to obtain a representative enough dataset.

The current approach to solve this problem consist in building a very large and heterogeneous dataset, as described in [5]. By taking such an approach, the steganalyst expects that the trained classifier (usually a convolutional neural network) will learn a collection of features that are universal to all images and, consequently, good enough to classify images taken under conditions different from those of the training set. Although this approach is often successful, we think that it is convenient to test other solutions to the problem. In this paper, we explore an alternative approach.

The proposed approach is based on the ideas of [16], which are extended here to detect samples that lead to classification inconsistencies. Thus, the suggested method stems from obtaining

additional training and testing sets by sequential random data embedding. Those additional sets are used here to detect inconsistencies in the classification. We present a method in the context of batch steganography [11], that is, when we are analyzing a set of images from a suspicious source.

The rest of this paper is organized as follows. Section 2 introduces some relevant concepts that are used in the proposed method. Section 3 presents the proposed method. Experimental results obtained with the proposed method for different image databases, embedding algorithms and steganalytic classifiers (including CSM cases) are presented in Section 4. Finally, Section 5 summarizes the conclusions and suggests some directions for further research.

2 PRELIMINARIES

We consider a targeted scenario in which the embedding algorithm and the approximate embedding rate –but not the secret key– are assumed to be known (at least approximately) by the steganalyst. Using the same steganographic algorithm and embedding bit rate, new (random) data can be hidden into any image with a different (random) secret key. Given a set of cover images, they can be used to build a training database by embedding random data to obtain a training database consisting of a half of cover and a half of stego images. This set is called A^{train}. If a feature extraction-based machine learning algorithm is applied (not all the machine learning algorithms need feature extraction [3]), we need to extract the features of the images. The usual methodology in machine learning-based steganalysis is to use the set A^{train} to train a classifier. Then, this classifier can be used to classify a testing set A^{test}, that is, a set of images for which we do not have *a priori* information whether they are cover or stego.

The proposed methodology uses an additional set, B^{train}, defined as suggested in [16]. The set B^{train} is the result of hiding random data into all the images of the set A^{train} using the targeted embedding algorithm, the approximate embedding bit rate and random keys. As a result, we have a set A^{train}, which contains cover and stego images, and a set B^{train}, which contains stego and "double stego" images.

Now, we introduce the following notation: let α_i be a sample from the set A^{train} and β_i be the corresponding sample from the set B^{train}, whereby $\beta_i = \text{Embed}(\alpha_i, \text{Bitrate})$. "Embed" stands for embedding a random message, using a random key and the targeted steganographic algorithm, and "Bitrate" is the known (or approximated) embedding bit rate.

Similarly, from the images in A^{test}, we build an additional set B^{test} following the same procedure: a_i and b_i stand for samples of the training sets A^{test} and B^{test}, respectively, with $b_i = \text{Embed}(a_i, \text{Bitrate})$. The only difference with respect to the training sets is that we do not know the classes (labels) of the images of the testing sets. In other words, we know that A^{test} possibly contains both cover and stego images, and that B^{test} possibly contains stego and "double stego" images, but we do not know the class of each image.

Finally, we assume that there is a classifier $\hat{f}_A$ (and a feature extractor if needed) that can split images into cover ($\mathcal{C}_A$) and stego ($\mathcal{S}_A$) classes with an acceptable probability of error. Similarly, we assume that we have another classifier $\hat{f}_B$ that can split images into stego ($\mathcal{S}_B$) and "double stego" ($\mathcal{D}_B$) classes,

Table 1: Number of pixels modified by ±1 and ±2 for 1,000 images after the first and the second embeddings. "ALGO"/"BR": embedding algorithm and bit rate (bpp)

		1 embedding		2 embeddings	
ALGO	BR	±1	±2	±1	±2
HILL	0.4	22,582,706	0	33,993,485	2,819,705
HILL	0.2	9,897,485	0	16,112,459	933,376
UNIWARD	0.4	19,509,940	0	32,748,639	1,563,635
UNIWARD	0.2	8,523,446	0	15,139,023	477,200
LSBM	0.2	27,528,954	0	49,277,814	1,439,498

The assumption of the existence of $\hat{f}_B$ that can split images into stego ($\mathcal{S}_B$) and "double stego" ($\mathcal{D}_B$) classes needs some discussion. After all, both $\mathcal{S}_B$ and $\mathcal{D}_B$ classes are formed by stego images with more or less information hidden into them. Usually, in the spatial domain, steganographic algorithms embed information by carrying out a ±1 operation in some specific pixels. In a second embedding, the steganographic algorithm may choose an already modified pixel to hide additional information. Thus, in addition to ±1 changes, there is some probability of a ±2 operation for a few pixels. In the particular case of adaptive embedding, a probability map indicates the areas that will be selected for hiding information. These probability maps are quite similar for the cover and stego versions of the same image. Therefore, the algorithm tends to hide information in the same pixels. This increases the differences between the features of stego and "double stego" images. These differences become more detectable with greater embedding ratios. One can conclude that the patterns of pixels (and its neighbours) generated after the second embedding will be different from those of a single embedding, and a good enough classifier can take advantage of those differences. In Table 1, the number of ±1 and ±2 variations after embedding messages with different algorithms and bit rates in 1,000 images randomly selected from the BOSS base are shown. We have included an experiment with LSB matching to show that even with non-adaptive steganography, the number of ±2 variations is not negligible. It can be observed that the number of ±2 variations is relatively large and and that the final number of ±1 changes is higher after the second embedding. These two factors help the classifier to split stego and "double stego" images. Even in the case of LSB matching, which does not use a probability map that forces the algorithm to hide data in the same positions, the number of ±2 variations is quite high. To analyze the relevance of ±2 changes for the classification, we trained a classifier $\hat{f}_B$ using the BOSS database and the HILL embedding algorithm with a bit rate of 0.4 bits per pixel (bpp). We obtained a classification error of 0.2770. Next, we trained the classifier with the same images after replacing the ±2 changes by their respective ±1 values. In this case, we obtained an error of 0.3160, which is slightly worse. Therefore, it can be seen that, although the influence of ±2 changes in the classification is very significant, the increase in the number of ±1 changes is enough to split both classes.

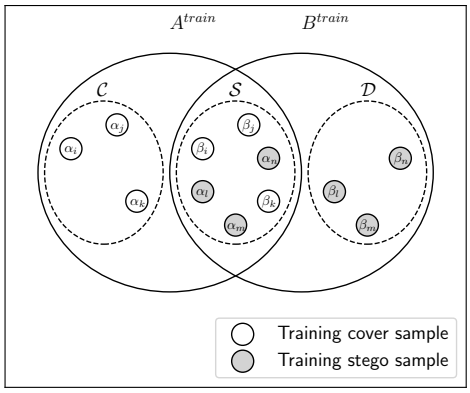

(a) A^{train} and B^{train} sets

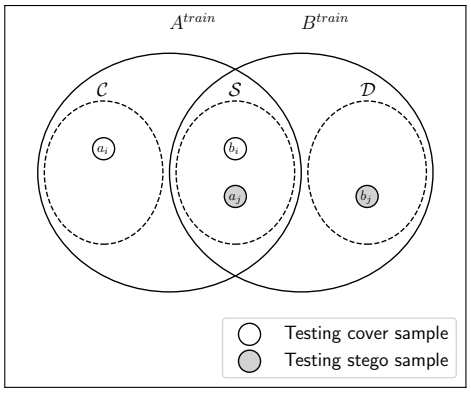

(b) Consistent predictions

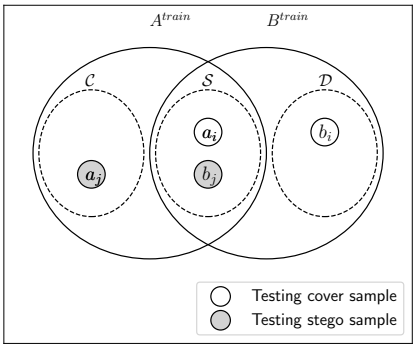

(c) Undetectable inconsistencies

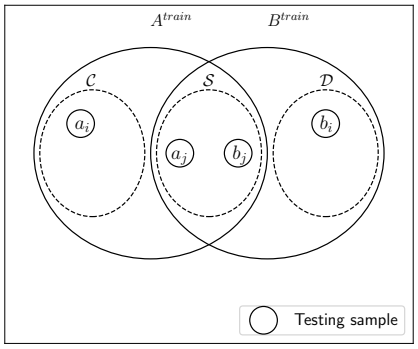

(d) Some F_1-detectable inconsistencies

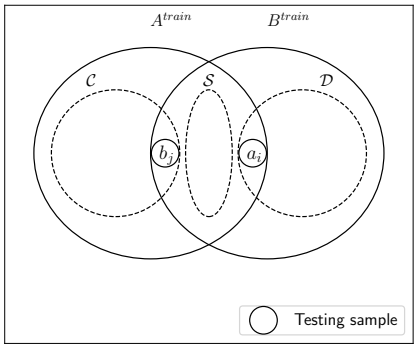

(e) F_2-detectable inconsistencies

Fig. 1. Graphical representation of the proposed method

3 PROPOSED METHOD

This section outlines the method proposed to detect the number of inconsistencies occurred during classification. We also propose a mechanism to predict the error incurred by the classifier based on the number of such inconsistencies.

Usually, in machine learning-based steganalysis, when we know the embedding algorithm and the approximate embedding rate, the testing set is expected to be classified with some (hopefully low) probability of error [7]. If this idea is extended to the sets introduced in the previous section, we have a tool that can be used to detect inconsistencies in classification. Since there is a bijection between the elements of A^{test} and B^{test}, if an image is classified as cover using $\hat{f}_A$, the corresponding image in B^{test} should be classified as stego (not "double stego") using $\hat{f}_B$. Similarly, if an image in A^{test} is classified as stego using $\hat{f}_A$, we expect the same image in B^{test} to be classified as "double stego" if we use $\hat{f}_B$. We call "inconsistency" to a classification result that does not meet these requirements.

The classification constraints described above are used to define *filters*. The filter described in the previous paragraph is denoted as F_1, and consists in classifying a_i using $\hat{f}_A$ and b_i using $\hat{f}_B$ to check whether the two classification results are consistent:

$$F_1(i) \equiv \begin{cases} \text{If } \hat{f}_A(a_i) = \mathcal{S}_A, & \text{If } (\hat{f}_B(b_i) \neq \mathcal{D}_B) \\ & \text{then output "inconsistency",} \\ \text{Otherwise,} & \text{If } (\hat{f}_B(b_i) \neq \mathcal{S}_B) \\ & \text{then output "inconsistency".} \end{cases}$$

In Fig.1a, we can see a graphical representation of the classes. A consistent classification is represented in Fig.1b. In Fig.1d, we can see different inconsistencies that can be detected with the filter F_1.

Now, we can consider the case in which $\hat{f}_A$ is used to classify $a_i \in A^{\text{test}}$ and the classification result is stego. If we classify $a_i \in A^{\text{test}}$ using $\hat{f}_B$, we expect that it is classified also as stego (not as "double stego"). If a_i is classified as stego using $\hat{f}_A$ and as "double stego" by $\hat{f}_B$, there is an inconsistency. In fact, if a_i corresponds to a cover image, it would not be consistent that a_i is classified by $\hat{f}_B$ as "double stego" either. Hence, for any image a_i in A^{test}, the output of $\hat{f}_B$ taking a_i as input must be always stego and never "double stego". The same idea can be applied to inconsistencies for the set B^{test}. If we use $\hat{f}_A$ to classify any sample $b_i \in B^{\text{test}}$, we expect b_i to be classified as stego (and never as cover). This kind of filter is

denoted as F_2 (represented in Fig.1e):

$$F_2(i) \equiv \begin{cases} \text{If } \hat{f}_B(a_i) \neq \mathcal{S}_B, & \text{then output "inconsistency",} \\ \\ \text{If } \hat{f}_A(b_i) \neq \mathcal{S}_A, & \text{then output "inconsistency".} \end{cases}$$

Note that there is a case that cannot be detected with these filters: an image that is misclassified by all the classifiers. A graphical representation of this case is provided in Fig.1c.

4 EXPERIMENTAL RESULTS

The experimental validation of the method has been performed with different datasets selecting images from the following databases:

- The BOSS database is the set of images from the Break Our Steganographic System! competition [1]. This database is formed by 10,000 cover images taken with seven different cameras, with a size of 512×512 pixels. For JPEG experiments, we have compressed the images to qualities 75 and 95. In these cases, we refer to the datasets as BOSS-J75 and BOSS-J95, respectively.
- The BOWS2 database is the set of images from the Break Our Watermarking System 2nd Ed. competition [2]. This database is formed by 10,000 cover images with a size of 512×512 pixels. For JPEG experiments, we have compressed the images to qualities 75 and 95. In these cases, we refer to the datasets as BOWS2-J75 and BOWS2-J95, respectively.
- The ALASKA database is the set of images from the Alaska competition [5]. This database is formed by 50,000 cover images with different sizes. For our experiments, we have selected 10,000 images randomly and we have cropped the center with a size of 512×512 pixels, and then converted them to gray scale. For JPEG experiments, we compressed the cropped images to qualities 75 and 95. In these cases, we refer to the datasets as ALASKA-J75 and ALASKA-J95, respectively.

For the experiments with SRNet [3], all these datasets have been resized to 256×256 pixels.

All the databases were randomly separated into two sets: a set for training and a set for testing. All the experiments, but Experiment 2 in Table 2, use 9,500 images for training. Experiment 2 uses 5,000 images for training. The number of images used for testing varies among different experiments and it is provided in the different tables. These sets have been formed by the original cover images and the same images with an embedded message, using a random key. In this way, we have tested the CSM problem by using a training set from a database and a testing set from another one.

The experiments detailed below have been carried out for three different spatial domain steganographic algorithms: UNIversal WAvelet Relative Distortion (UNIWARD) [10], HIgh-pass, Low-pass, and Low-pass (HILL) [17] and LSB matching (LSBM) [21]; and for two different transformed domain steganographic algorithms: UED [9] and J-UNIWARD [10]. We were mainly interested in the results of the state-of-the-art algorithms, but we have also performed experiments using LSB matching to have a reference of a non-adaptive algorithm.

For these experiments, we have used a different random key for each stego image. The experiments have been performed using the same algorithm and embedding bit rate for the training and the testing sets unless explicitly noted otherwise. Thus, the proposed scenario is for a known algorithm and known embedding rate attack. To analyze the proposed approach, we have used the well known Rich Models (RM) framework [7] for the spatial domain and Gabor Filter Residuals (GFR) [22] for the transformed domain, with Ensemble Classifiers (EC) [13]. These classifiers meet the requirements introduced in Section 3, i.e., they make it possible to classify the sets A^{test} (as C_A and $\mathcal{S}_A$) and B^{test} (as $\mathcal{S}_B$ and $\mathcal{D}_B$) for UNIWARD, HILL, LSBM, UED and similar algorithms. When using RM+EC, we do not expect the proposed approach to work with algorithms designed to overcome this framework, such as [15], because the proposed method depends on the underlying classifier.

We have also performed some experiments using the state-of-the-art convolutional neural network (CNN) described in [3].

4.1 Classifier Inconsistencies

The results obtained detecting inconsistencies are presented in this section. In Tables 2-8, the results for different experiments are shown. The first column indicates the experiment number (used for references along the text). The first few columns show the algorithm and bit rate used for embedding, the databases used for training and for testing, the number of cover and stego images contained by the testing set, and the method used for classification. For example, the first row of the first experiment shows the results obtained using images from BOSS for training and images from the same database for testing (500 cover and 500 stego images), for HILL steganography with a 0.4 bpp embedding bit rate, using Rich Models with Ensemble Classifiers as the classification method. The results are computed first without applying any filter and next with the proposed filters. The column error (Err) is the result of the classification error using the reported method. This error is computed as:

$$\text{Err} = \frac{\text{FP} + \text{FN}}{\text{FP} + \text{FN} + \text{TP} + \text{TN}},$$

where TP are the true positives, TN the true negatives, FP the false positives and FN the false negatives. These values are also provided in Tables 2-8.

When the filters are applied, we also show the number of inconsistencies (INC) obtained during the classification, and which of those correspond to images classified by $\hat{f}_A$ as cover (INC_C) or as stego (INC_S). When there is no CSM (for example, in the first row of Experiment 1-A of Table 2) the number of inconsistencies is quite lower compared to the cases with CSM (e.g. the first rows of Experiments 1-B and 1-C of Table 2).

It can also be observed that the number of inconsistencies increases with lower embedding bit rates (Experiment 5 of Table 4). This occurs because the proposed method does not only reveal if there is CSM, but whether the classifier is working well with the testing database or not. This information can be used to make a good prediction about he classification errors, as detailed below.

4.2 Prediction of the Classification Error

In this section, we show how to carry out a prediction of the classification error. For this purpose, we assume that the standard steganalyzer is classifying randomly the samples that are not well

Table 2: Classification results for standard RM+EC (without filters) and for the proposed method (with filters). "N": number of experiment, "ALGO": name of the embedding algorithm and embedding bit rate (bpp), "DBs": training/testing databases, "C/S": number of cover and stego images in the testing set , "CLF": classification method used, "Err": true classification error, {"TP", "TN", "FP", "FN"}: true and false positives and negatives, "INC": number of inconsistencies, "INC_C": number of inconsistencies for images predicted as cover, and "INC_S": number of inconsistencies for images predicted as stego

					STANDARD					PROPOSED								
N	ALGO	DBs	C/S	CLF	Err	TP	TN	FP	FN	Err_{pred}	Err	TP	TN	FP	FN	INC	INC_C	INC_S
	HILL-0.40	BOSS/BOSS	500/500	RM+EC	**0.2440**	398	358	142	102	**0.2410**	0.1564	214	223	41	40	482	197	285
	HILL-0.40	BOSS/BOSS	500/250	RM+EC	**0.2573**	199	358	142	51	**0.2407**	0.1491	108	223	41	17	361	169	192
1-A	HILL-0.40	BOSS/BOSS	500/0	RM+EC	**0.2840**	0	358	142	0	**0.2360**	0.1553	0	223	41	0	236	135	101
	HILL-0.40	BOSS/BOSS	250/500	RM+EC	**0.2320**	398	178	72	102	**0.2420**	0.1628	214	110	23	40	363	130	233
	HILL-0.40	BOSS/BOSS	0/500	RM+EC	**0.2040**	398	0	0	102	**0.2460**	0.1575	214	0	0	40	246	62	184
	HILL-0.40	BOSS/BOWS2	500/500	RM+EC	**0.4530**	493	54	446	7	**0.4365**	0.7087	21	16	89	1	873	44	829
	HILL-0.40	BOSS/BOWS2	500/250	RM+EC	**0.6027**	244	54	446	6	**0.4233**	0.7826	9	16	89	1	635	43	592
1-B	HILL-0.40	BOSS/BOWS2	500/0	RM+EC	**0.8920**	0	54	446	0	**0.3950**	0.8476	0	16	89	0	395	38	357
	HILL-0.40	BOSS/BOWS2	250/500	RM+EC	**0.3067**	493	27	223	7	**0.4473**	0.6203	21	9	48	1	671	24	647
	HILL-0.40	BOSS/BOWS2	0/500	RM+EC	**0.0140**	493	0	0	7	**0.4780**	0.0455	21	0	0	1	478	6	472
	HILL-0.40	BOSS/ALASKA	500/500	RM+EC	**0.4810**	369	150	350	131	**0.4750**	0.2600	19	18	11	2	950	261	689
	HILL-0.40	BOSS/ALASKA	500/250	RM+EC	**0.5453**	191	150	350	59	**0.4727**	0.2927	11	18	11	1	709	190	519
1-C	HILL-0.40	BOSS/ALASKA	500/0	RM+EC	**0.7000**	0	150	350	0	**0.4710**	0.3793	0	18	11	0	471	132	339
	HILL-0.40	BOSS/ALASKA	250/500	RM+EC	**0.4027**	369	79	171	131	**0.4787**	0.1875	19	7	4	2	718	201	517
	HILL-0.40	BOSS/ALASKA	0/500	RM+EC	**0.2620**	369	0	0	131	**0.4790**	0.0952	19	0	0	2	479	129	350
	HILL-0.40	BOSS/BOSS	5000/5000	RM+EC	**0.2515**	3763	3722	1278	1237	**0.2519**	0.1477	2047	2183	341	392	5037	2384	2653
	HILL-0.40	BOSS/BOSS	5000/2500	RM+EC	**0.2511**	1895	3722	1278	605	**0.2499**	0.1426	1034	2183	341	194	3748	1950	1798
2-A	HILL-0.40	BOSS/BOSS	5000/0	RM+EC	**0.2556**	0	3722	1278	0	**0.2476**	0.1351	0	2183	341	0	2476	1539	937
	HILL-0.40	BOSS/BOSS	2500/5000	RM+EC	**0.2483**	3763	1875	625	1237	**0.2541**	0.1510	2047	1085	165	392	3811	1635	2176
	HILL-0.40	BOSS/BOSS	0/5000	RM+EC	**0.2474**	3763	0	0	1237	**0.2561**	0.1607	2047	0	0	392	2561	845	1716
	HILL-0.40	BOSS/BOWS2	5000/5000	RM+EC	**0.4328**	4814	858	4142	186	**0.4426**	0.6429	227	183	720	18	8852	843	8009
	HILL-0.40	BOSS/BOWS2	5000/2500	RM+EC	**0.5640**	2412	858	4142	88	**0.4317**	0.7090	115	183	720	6	6476	757	5719
2-B	HILL-0.40	BOSS/BOWS2	5000/0	RM+EC	**0.8284**	0	858	4142	0	**0.4097**	0.7973	0	183	720	0	4097	675	3422
	HILL-0.40	BOSS/BOWS2	2500/5000	RM+EC	**0.2980**	4814	451	2049	186	**0.4536**	0.5460	227	89	362	18	6804	530	6274
	HILL-0.40	BOSS/BOWS2	0/5000	RM+EC	**0.0372**	4814	0	0	186	**0.4755**	0.0735	227	0	0	18	4755	168	4587
	HILL-0.40	BOSS/ALASKA	5000/5000	RM+EC	**0.4826**	3641	1533	3467	1359	**0.4764**	0.4386	146	119	147	60	9528	2713	6815
	HILL-0.40	BOSS/ALASKA	5000/2500	RM+EC	**0.5521**	1826	1533	3467	674	**0.4750**	0.4693	80	119	147	29	7125	2059	5066
2-C	HILL-0.40	BOSS/ALASKA	5000/0	RM+EC	**0.6934**	0	1533	3467	0	**0.4734**	0.5526	0	119	147	0	4734	1414	3320
	HILL-0.40	BOSS/ALASKA	2500/5000	RM+EC	**0.4123**	3641	767	1733	1359	**0.4777**	0.3970	146	56	73	60	7165	2010	5155
	HILL-0.40	BOSS/ALASKA	0/5000	RM+EC	**0.2718**	3641	0	0	1359	**0.4794**	0.2913	146	0	0	60	4794	1299	3495

represented by the classification model or by the training set. For example, in a balanced case with the same number of cover and stego images, a classifier that makes a classification error of $R\%$, is possibly having trouble with $2R\%$ of the samples of testing set, but it is providing the correct class for half of the "difficult" samples by chance. The images belonging to these $2R\%$ samples of the testing set are more likely to produce inconsistencies than those for which the classifier succeeds. For this reason, the number of inconsistencies tends to be similar to two times the number of errors produced by the standard classifier (without using filters). This fact can be observed in Table 2. Note that, in the balanced case, INC_C is roughly two times the number of FN (obtained without filters) and INC_S is roughly two times the number of FP (also without filters).

This prediction makes it possible to approximate the classification error of the testing set with the standard classifier using the following expression:

$$\mathrm{Err}_{\mathrm{pred}} = \frac{\mathrm{INC}}{2\,|A^{\mathrm{test}}|},$$

where $|\cdot|$ denotes the cardinality of a set. A more general expression that can be applied in non-balanced cases is left for the future research.

Tables 2-8 show the accuracy of the predicted classification error as compared to the true classification error. Please note that the predicted error can be computed without any knowledge of the true type (stego or cover) of the testing images, whereas the true classification error is computed using the true type of each image.

We have carried out experiments with different ratios of cover and stego images (Experiments 1-2 in Table 2, and 3-4 in Table 3). In the balanced case (500/500), the predicted error ($\mathrm{Err}_{\mathrm{pred}}$) is very close to the true classification error (Err). However, in the case of unbalanced number of cover and stego images, the predicted classification error is not that close to the real value, but it is close to the true classification error obtained with a balanced testing set.

Note that, due to the proposed formula, the prediction of the classification error will always be between 0 and 0.5. Therefore, a classifier that does not work for a given testing set would yield a prediction of the classification error about 0.5. In unbalanced experiments, we can obtain true classification errors above 0.5, such as in the third row of the Experiment 1-C (Table 2), with an error of 0.7000. Our prediction is 0.4787 indicating that the classifier is random guessing with this testing set. A similar situation occurs with apparently good classification results, as in the last row of Experiment 1-B (Table 2). The classification error is 0.0140, whereas the prediction of the classification error is 0.4790. Note that the

Table 3: Classification results for standard RM+EC (without filters) and for the proposed method (with filters). Symbols and abbreviations have the same meaning as in Table 2.

					STANDARD					PROPOSED								
N	ALGO	DBs	C/S	CLF	Err	TP	TN	FP	FN	Err_{pred}	Err	TP	TN	FP	FN	INC	INC_C	INC_S
	UNIW-0.40	BOSS/BOSS	500/500	RM+EC	**0.2030**	419	378	122	81	**0.1965**	0.1203	257	277	40	33	393	149	244
	UNIW-0.40	BOSS/BOSS	500/250	RM+EC	**0.2240**	204	378	122	46	**0.1947**	0.1201	126	277	40	15	292	132	160
3-A	UNIW-0.40	BOSS/BOSS	500/0	RM+EC	**0.2440**	0	378	122	0	**0.1830**	0.1262	0	277	40	0	183	101	82
	UNIW-0.40	BOSS/BOSS	250/500	RM+EC	**0.1920**	419	187	63	81	**0.1993**	0.1175	257	141	20	33	299	94	205
	UNIW-0.40	BOSS/BOSS	0/500	RM+EC	**0.1620**	419	0	0	81	**0.2100**	0.1138	257	0	0	33	210	48	162
	UNIW-0.40	BOSS/BOW2	500/500	RM+EC	**0.4330**	485	82	418	15	**0.3830**	0.6795	43	32	157	2	766	63	703
	UNIW-0.40	BOSS/BOW2	500/250	RM+EC	**0.5667**	243	82	418	7	**0.3573**	0.7430	23	32	157	2	536	55	481
3-B	UNIW-0.40	BOSS/BOW2	500/0	RM+EC	**0.8360**	0	82	418	0	**0.3110**	0.8307	0	32	157	0	311	50	261
	UNIW-0.40	BOSS/BOW2	250/500	RM+EC	**0.2973**	485	42	208	15	**0.4080**	0.5870	43	14	79	2	612	41	571
	UNIW-0.40	BOSS/BOW2	0/500	RM+EC	**0.0300**	485	0	0	15	**0.4550**	0.0444	43	0	0	2	455	13	442
	UNIW-0.40	BOSS/ALASKA	500/500	RM+EC	**0.4830**	397	120	380	103	**0.4805**	0.4103	12	11	16	0	961	212	749
	UNIW-0.40	BOSS/ALASKA	500/250	RM+EC	**0.5680**	204	120	380	46	**0.4780**	0.4848	6	11	16	0	717	155	562
3-C	UNIW-0.40	BOSS/ALASKA	500/0	RM+EC	**0.7600**	0	120	380	0	**0.4730**	0.5926	0	11	16	0	473	109	364
	UNIW-0.40	BOSS/ALASKA	250/500	RM+EC	**0.3853**	397	64	186	103	**0.4867**	0.2000	12	4	4	0	730	163	567
	UNIW-0.40	BOSS/ALASKA	0/500	RM+EC	**0.2060**	397	0	0	103	**0.4880**	0.0000	12	0	0	0	488	103	385
	LSBm-0.10	BOSS/BOSS	500/500	RM+EC	**0.0860**	458	456	44	42	**0.0780**	0.0592	396	398	24	26	156	74	82
	LSBm-0.10	BOSS/BOSS	500/250	RM+EC	**0.0920**	225	456	44	25	**0.0767**	0.0661	195	398	24	18	115	65	50
4-A	LSBm-0.10	BOSS/BOSS	500/0	RM+EC	**0.0880**	0	456	44	0	**0.0780**	0.0569	0	398	24	0	78	58	20
	LSBm-0.10	BOSS/BOSS	250/500	RM+EC	**0.0867**	458	227	23	42	**0.0760**	0.0597	396	202	12	26	114	41	73
	LSBm-0.10	BOSS/BOSS	0/500	RM+EC	**0.0840**	458	0	0	42	**0.0780**	0.0616	396	0	0	26	78	16	62
	LSBm-0.10	BOSS/BOW2	500/500	RM+EC	**0.1270**	478	395	105	22	**0.0975**	0.0882	374	360	56	15	195	42	153
	LSBm-0.10	BOSS/BOW2	500/250	RM+EC	**0.1520**	241	395	105	9	**0.0780**	0.0979	211	360	56	6	117	38	79
4-B	LSBm-0.10	BOSS/BOW2	500/0	RM+EC	**0.2100**	0	395	105	0	**0.0840**	0.1346	0	360	56	0	84	35	49
	LSBm-0.10	BOSS/BOW2	250/500	RM+EC	**0.1227**	478	180	70	22	**0.1093**	0.0939	374	157	40	15	164	30	134
	LSBm-0.10	BOSS/BOW2	0/500	RM+EC	**0.0440**	478	0	0	22	**0.1110**	0.0386	374	0	0	15	111	7	104
	LSBm-0.10	BOSS/ALASKA	500/500	RM+EC	**0.4730**	399	128	372	101	**0.4500**	0.5000	26	24	45	5	900	200	700
	LSBm-0.10	BOSS/ALASKA	500/250	RM+EC	**0.5667**	197	128	372	53	**0.4440**	0.5595	13	24	45	2	666	155	511
4-C	LSBm-0.10	BOSS/ALASKA	500/0	RM+EC	**0.7440**	0	128	372	0	**0.4310**	0.6522	0	24	45	0	431	104	327
	LSBm-0.10	BOSS/ALASKA	250/500	RM+EC	**0.3867**	399	61	189	101	**0.4580**	0.4127	26	11	21	5	687	146	541
	LSBm-0.10	BOSS/ALASKA	0/500	RM+EC	**0.2020**	399	0	0	101	**0.4690**	0.1613	26	0	0	5	469	96	373

Table 4: Experiments with low bit rates. Symbols and abbreviations have the same meaning as in Table 2.

					STANDARD					PROPOSED								
N	ALGO	DBs	C/S	CLF	Err	TP	TN	FP	FN	Err_{pred}	Err	TP	TN	FP	FN	INC	INC_C	INC_S
5	HILL-0.20	BOSS/BOSS	500/500	RM+EC	**0.3530**	350	297	203	150	**0.3545**	0.2509	106	112	36	37	709	298	411
	HILL-0.20	BOSS/BOW2	500/500	RM+EC	**0.4850**	474	41	459	26	**0.4875**	0.7200	4	3	15	3	975	61	914
	UNIW-0.20	BOSS/BOSS	500/500	RM+EC	**0.3360**	352	312	188	148	**0.3205**	0.1922	145	145	34	35	641	280	361
	UNIW-0.20	BOSS/BOW2	500/500	RM+EC	**0.4650**	485	50	450	15	**0.4620**	0.5658	19	14	40	3	924	48	876

Table 5: Experiments training with images from other databases. Symbols and abbreviations have the same meaning as in Table 2.

					STANDARD					PROPOSED								
N	ALGO	DBs	C/S	CLF	Err	TP	TN	FP	FN	Err_{pred}	Err	TP	TN	FP	FN	INC	INC_C	INC_S
	HILL-0.40	BOWS2/BOWS2	500/500	RM+EC	**0.2060**	414	380	120	86	**0.1900**	0.1161	268	280	34	38	380	148	232
6-A	HILL-0.40	BOWS2/BOSS	500/500	RM+EC	**0.3140**	364	322	178	136	**0.3055**	0.2031	148	162	42	37	611	259	352
	HILL-0.40	BOWS2/ALASKA	500/500	RM+EC	**0.4710**	363	166	334	137	**0.4685**	0.3968	20	18	17	8	937	277	660
	HILL-0.40	ALASKA/ALASKA	500/500	RM+EC	**0.2950**	378	327	173	122	**0.2895**	0.1354	177	187	31	26	579	236	343
6-B	HILL-0.40	ALASKA/BOSS	500/500	RM+EC	**0.4110**	387	202	298	113	**0.3905**	0.2466	78	87	27	27	781	201	580
	HILL-0.40	ALASKA/BOWS2	500/500	RM+EC	**0.3710**	273	356	144	227	**0.3730**	0.2756	81	103	29	41	746	439	307

predicted classification error is correct, as far as the classifier is not working in these conditions, as evident from the balanced case (first row of Experiment 1-B). The reason why the classification error is so small in the all-stego case is that the output of the classifier is stego for almost all images, which works by chance when all testing images are stego.

Table 6: Experiments using the SRNet convolutional neural network. Symbols and abbreviations have the same meaning as in Table 2.

					STANDARD					PROPOSED								
N	ALGO	DBs	C/S	CLF	Err	TP	TN	FP	FN	Err_{pred}	Err	TP	TN	FP	FN	INC	INC_C	INC_S
	HILL-0.40	BOSS/BOSS	500/500	SRNET	**0.2520**	434	314	186	66	**0.2635**	0.1057	216	207	35	15	527	158	369
7-A	HILL-0.40	BOSS/BOWS2	500/500	SRNET	**0.2600**	447	293	207	53	**0.2855**	0.1235	178	198	33	20	571	128	443
	HILL-0.40	BOSS/ALASKA	500/500	SRNET	**0.3840**	441	175	325	59	**0.3825**	0.2128	75	110	22	28	765	96	669
	HILL-0.40	BOWS2/BOWS2	500/500	SRNET	**0.2670**	437	296	204	63	**0.2720**	0.1272	184	214	35	23	544	122	422
7-B	HILL-0.40	BOWS2/BOSS	500/500	SRNET	**0.3570**	452	191	309	48	**0.3250**	0.2000	156	124	62	8	650	107	543
	HILL-0.40	BOWS2/ALASKA	500/500	SRNET	**0.3880**	319	293	207	181	**0.3805**	0.2218	80	106	28	25	761	343	418
	HILL-0.40	ALASKA/ALASKA	500/500	SRNET	**0.3940**	324	282	218	176	**0.3910**	0.2156	76	95	34	13	782	350	432
7-C	HILL-0.40	ALASKA/BOWS2	500/500	SRNET	**0.3930**	438	169	331	62	**0.3930**	0.2150	77	91	35	11	786	129	657
	HILL-0.40	ALASKA/BOSS	500/500	SRNET	**0.3900**	386	224	276	114	**0.4120**	0.2955	68	56	43	9	824	273	551

Table 7: Experiments with unknown bitrate (SSM). Symbols and abbreviations have the same meaning as in Table 2.

					STANDARD					PROPOSED								
N	ALGO	DBs	C/S	CLF	Err	TP	TN	FP	FN	Err_{pred}	Err	TP	TN	FP	FN	INC	INC_C	INC_S
	HILL-0.40/0.20	BOSS/BOSS	500/500	RM+EC	**0.2850**	418	297	203	82	**0.4200**	0.2625	6	112	36	6	840	261	579
	HILL-0.40/0.30	BOSS/BOSS	500/500	RM+EC	**0.2450**	413	342	158	87	**0.3470**	0.1667	84	171	35	16	694	242	452
8	HILL-0.40/0.40	BOSS/BOSS	500/500	RM+EC	**0.2440**	398	358	142	102	**0.2410**	0.1564	214	223	41	40	482	197	285
	HILL-0.40/0.50	BOSS/BOSS	500/500	RM+EC	**0.2640**	344	392	108	156	**0.1880**	0.1538	250	278	35	61	376	209	167
	HILL-0.40/0.60	BOSS/BOSS	500/500	RM+EC	**0.2820**	312	406	94	188	**0.1800**	0.1422	242	307	33	58	360	229	131

Note that Experiment 2 (Table 2) is the same as Experiment 1 (Table 2) but using 10,000 images for training and 10,000 images for testing. This experiment was carried out to check if the results with 1,000 images are stable enough. We can see that, in both cases, the results are very similar.

In Experiments 3 and 4 (Table 3), the results obtained for the embedding algorithms UNIWARD and LSB matching are shown, and the accuracy of the predicted classification error is similar to that of Table 2. Comparable results are also obtained with low embedding bit rates, as it can be observed in Experiment 5 (Table 4) for the algorithms HILL and UNIWARD with 0.2 bpp.

In the previous experiments, the database used for training is BOSS. In Experiment 6 (Table 5), we show the results obtained using images from other databases for training. More precisely, we use BOWS2 and ALASKA in the training set. As it can be observed, the results are comparable in terms of the accuracy of the prediction of the classification error.

In Experiment 7 (Table 6), the results using the SRNet [3] classification method are presented, and different training databases are used. Again, the prediction of the classification errors is accurate.

Experiment 8 (Table 7) presents the classification results in case of SSM. In this case, the testing set is embedded with HILL and 0.40 bpb, and the embedding bit rate of the training set varies between 0.20 and 0.60 bpp. When a wrong embedding bit rate is chosen, the prediction of the classification error is less accurate. The reason for this mismatch is that a wrong embedding rate is used to create the set B^{train} and, hence, the classifier $\hat{f}_B$ is not appropriate for the testing set. This problem will be addressed in our future work.

Finally, in Experiments 9 and 10 (Table 8), we show the results obtained for JPEG images compressed to qualities 75 and 95, respectively. In this case, we have used the embedding algorithms UED and J-UNIWARD, and the accuracy of the predicted classification error is consistent with that of the rest of the experiments.

As shown in the experiments, the proposed method works both if there is CSM and when it is too difficult to classify images with the underlying classifier in case of a too small embedding bit rate.

5 CONCLUSION

In this paper, a method for detecting inconsistencies in image steganalysis is presented. We show how the number of inconsistencies can be used to predict the classification error of the steganalytic method. The proposed approach has been tested for different steganalyzers, image databases, embedding algorithms and embedding bit rates, with and without CSM.

The results show how the classification error of a steganalytic method can be predicted without having access to the labels of the images in the testing set. The predicted classification error can be a very valuable information for a steganalyst, who can decide how to proceed when the predicted classification error is too large. In such a case, increasing the training set in order to improve the classification accuracy could be one of the alternatives to be considered.

The proposed method is intended to be used in batch steganography. Nevertheless, even for a single testing image, this approach makes it possible to detect if the classification is inconsistent. In such a case, the classifier should not be used to classify that image. As future work, it would be worth analyzing how to take profit of the proposed methodology when classifying single images. Finally, in case of *stego source mismatch* (e.g. when the embedding bit rate is not known accurately) the prediction of the classification is not reliable. Possible approaches to deal with this problem will be addressed in our future research.

Table 8: Experiments with JPEG steganography. Symbols and abbreviations have the same meaning as in Table 2.

					STANDARD					PROPOSED							
N	ALGO	DBs	C/S	CLF	Err	TP	TN	FP	FN	Err_{pred}	Err	TP	TN	FP	FN	INC	INC_C	INC_S
	UED-0.40	BOSS-J75/BOSS-J75	500/500	GFR+EC	**0.0290**	480	491	9	20	**0.0315**	0.0267	452	460	8	17	63	34	29
	UED-0.40	BOSS-J75/BOWS2-J75	500/500	GFR+EC	**0.0300**	481	489	11	19	**0.0355**	0.0215	450	459	6	14	71	35	36
9-A	UED-0.40	BOSS-J75/ALASKA-J75	500/500	GFR+EC	**0.2090**	348	443	57	152	**0.2315**	0.1899	204	231	29	73	463	291	172
	J-UNIW-0.40	BOSS-J75/BOSS-J75	500/500	GFR+EC	**0.0820**	446	472	28	54	**0.0910**	0.0819	362	389	22	45	182	92	90
	J-UNIW-0.40	BOSS-J75/BOWS2-J75	500/500	GFR+EC	**0.1000**	445	455	45	55	**0.0990**	0.0998	348	374	37	43	198	93	105
	UED-0.40	BOWS2-J75/BOWS2-J75	500/500	GFR+EC	**0.0240**	490	486	14	10	**0.0340**	0.0193	452	462	9	9	68	25	43
	UED-0.40	BOWS2-J75/BOSS-J75	500/500	GFR+EC	**0.0350**	487	478	22	13	**0.0305**	0.0309	452	458	19	10	61	23	38
9-B	UED-0.40	BOWS2-J75/ALASKA-J75	500/500	GFR+EC	**0.2070**	346	447	53	154	**0.2435**	0.1910	194	221	27	71	487	309	178
	J-UNIW-0.40	BOWS2-J75/BOWS2-J75	500/500	GFR+EC	**0.0970**	450	453	47	50	**0.0990**	0.0960	352	373	35	42	198	88	110
	J-UNIW-0.40	BOWS2-J75/BOSS-J75	500/500	GFR+EC	**0.0960**	466	438	62	34	**0.1165**	0.0769	346	362	38	21	233	89	144
	UED-0.40	ALASKA-J75/ALASKA-J75	500/500	GFR+EC	**0.0800**	456	464	36	44	**0.0955**	0.0581	375	387	20	27	191	94	97
9-C	UED-0.40	ALASKA-J75/BOSS-J75	500/500	GFR+EC	**0.0680**	453	479	21	47	**0.0805**	0.0536	385	409	16	29	161	88	73
	UED-0.40	ALASKA-J75/BOWS2-J75	500/500	GFR+EC	**0.0890**	442	469	31	58	**0.0925**	0.0847	363	383	24	45	185	99	86
	UED-0.40	BOSS-J95/BOSS-J95	500/500	GFR+EC	**0.1530**	430	417	83	70	**0.1310**	0.1220	319	329	47	43	262	115	147
	UED-0.40	BOSS-J95/BOWS2-J95	500/500	GFR+EC	**0.1900**	368	442	58	132	**0.1635**	0.1842	267	282	30	94	327	198	129
10-A	UED-0.40	BOSS-J95/ALASKA-J95	500/500	GFR+EC	**0.4310**	140	429	71	360	**0.4145**	0.4152	44	56	13	58	829	675	154
	J-UNIW-0.40	BOSS-J95/BOSS-J95	500/500	GFR+EC	**0.2280**	369	403	97	131	**0.2295**	0.2089	201	227	50	63	459	244	215
	J-UNIW-0.40	BOSS-J95/BOWS2-J95	500/500	GFR+EC	**0.2640**	324	412	88	176	**0.2560**	0.2295	183	193	37	75	512	320	192
	UED-0.40	BOWS2-J95/BOWS2-J95	500/500	GFR+EC	**0.1660**	414	420	80	86	**0.1525**	0.1640	285	296	47	67	305	143	162
	UED-0.40	BOWS2-J95/BOSS-J95	500/500	GFR+EC	**0.1690**	427	404	96	73	**0.1460**	0.1427	306	301	52	49	292	127	165
10-B	UED-0.40	BOWS2-J95/ALASKA-J95	500/500	GFR+EC	**0.4180**	154	428	72	346	**0.3995**	0.3980	53	68	22	58	799	648	151
	J-UNIW-0.40	BOWS2-J95/BOWS2-J95	500/500	GFR+EC	**0.2600**	366	374	126	134	**0.2380**	0.2481	194	200	71	59	476	249	227
	J-UNIW-0.40	BOWS2-J95/BOSS-J95	500/500	GFR+EC	**0.2460**	380	374	126	120	**0.2380**	0.2252	194	212	59	59	476	223	253
	UED-0.40	ALASKA-J95/ALASKA-J95	500/500	GFR+EC	**0.3040**	349	347	153	151	**0.2665**	0.2227	183	180	35	69	533	249	284
10-C	UED-0.40	ALASKA-J95/BOSS-J95	500/500	GFR+EC	**0.2350**	390	375	125	110	**0.2065**	0.2095	229	235	59	64	413	186	227
	UED-0.40	ALASKA-J95/BOWS2-J95	500/500	GFR+EC	**0.2400**	356	404	96	144	**0.2100**	0.2224	215	236	41	88	420	224	196

ACKNOWLEDGMENTS

This work was supported by the Spanish Government, in part under Grant RTI2018-095094-B-C22 “CONSENT”, and in part under Grant TIN2014-57364-C2-2-R “SMARTGLACIS.”

We gratefully acknowledge the support of NVIDIA Corporation with the donation of an NVIDIA TITAN Xp GPU card that has been used in this work.

REFERENCES

[1] P. Bas, T. Filler, and T. Pevný. 2011. "Break Our Steganographic System": The Ins and Outs of Organizing BOSS. In *Proceedings of the 13th International Conference on Information Hiding (IH'11)*. Springer-Verlag, 59–70.

[2] P. Bas and T. Furon. [n. d.]. "Break Our Watermarking System 2nd. Ed.". http://bows2.ec-lille.fr/. ([n. d.]). Accessed: July 2007.

[3] M. Boroumand, M. Chen, and J. Fridrich. 2019. Deep Residual Network for Steganalysis of Digital Images. *IEEE Transactions on Information Forensics and Security* 14, 5 (May 2019), 1181–1193.

[4] G. Cancelli, G. Doërr, M. Barni, and I. J. Cox. 2008. A Comparative Study of ±1 Steganalyzers. In *Multimedia Signal Processing, 2008 IEEE 10th Workshop on*. 791–796.

[5] R. Cogranne and P. Bas. [n. d.]. "Alaska". https://alaska.utt.fr. ([n. d.]). Accessed: March 2019.

[6] T. Denemark, V. Sedighi, V. Holub, R. Cogranne, and J. Fridrich. 2014. Selection-Channel-Aware Rich Model for Steganalysis of Digital Images. In *2014 IEEE International Workshop on Information Forensics and Security (WIFS)*. 48–53.

[7] J. Fridrich and J. Kodovský. 2012. Rich Models for Steganalysis of Digital Images. *IEEE Transactions on Information Forensics and Security* 7 (2012), 868–882.

[8] G. Gul and F. Kurugollu. 2011. A New Methodology in Steganalysis: Breaking Highly Undetectable Steganography (HUGO). In *Proceedings of the 13th International Conference on Information Hiding*. 71–84.

[9] L. Guo, J. Ni, and Y. Q. Shi. 2014. Uniform Embedding for Efficient JPEG Steganography. *IEEE Transactions on Information Forensics and Security* 9, 5 (May 2014), 814–825.

[10] V. Holub, J. Fridrich, and T. Denemark. 2014. Universal distortion function for steganography in an arbitrary domain. *EURASIP Journal on Information Security* 2014, 1 (2014), 1–13.

[11] A. D. Ker. 2007. Batch Steganography and Pooled Steganalysis. In *Proceedings of the 8th International Conference on Information Hiding (IH'06)*. Springer-Verlag, Berlin, Heidelberg, 265–281.

[12] A. D. Ker, P. Bas, R. Böhme, R. Cogranne, S. Craver, T. Filler, J. Fridrich, and T. Pevný. 2013. Moving Steganography and Steganalysis from the Laboratory into the Real World. In *Proceedings of the First ACM Workshop on Information Hiding and Multimedia Security*. 45–58.

[13] J. Kodovský, J. Fridrich, and V. Holub. 2012. Ensemble Classifiers for Steganalysis of Digital Media. *IEEE Transactions on Information Forensics and Security* 7, 2 (2012), 432–444.

[14] J. Kodovský, V. Sedighi, and J. Fridrich. 2014. Study of Cover Source Mismatch in Steganalysis and Ways to Mitigate its Impact. In *Proceedings of SPIE - The International Society for Optical Engineering*, Vol. 9028.

[15] S. Kouider, M. Chaumont, and W. Puech. 2013. Adaptive steganography by oracle (ASO). In *International Conference on Multimedia and Expo (ICME)*. IEEE, 1–6.

[16] Daniel Lerch-Hostalot and David Megías. 2016. Unsupervised steganalysis based on artificial training sets. *Engineering Applications of Artificial Intelligence* 50 (2016), 45–59.

[17] B. Li, M. Wang, J. Huang, and X. Li. 2014. A New Cost Function for Spatial Image Steganography. In *2014 IEEE International Conference on Image Processing (ICIP)*. 4206–4210.

[18] I. Lubenko and A. D. Ker. 2012. Going from Small to Large Data in Steganalysis. In *Media Watermarking, Security, and Forensics 2012 (Proceedings of SPIE - The International Society for Optical Engineering)*, Vol. 8303. 0M01–0M10.

[19] J. Pasquet, S. Bringay, and M. Chaumont. 2014. Steganalysis with Cover-Source Mismatch and a Small Learning Database. In *Proceedings of the 22nd European Signal Processing Conference (EUSIPCO)*. 2425–2429.

[20] Tomás Pevný. 2011. Detecting Messages of Unknown Length. *Proceedings of SPIE - The International Society for Optical Engineering* 7880 (2011), 78800T–78800T–12.

[21] T. Sharp. 2001. An Implementation of Key-Based Digital Signal Steganography. In *Information Hiding*. Lecture Notes in Computer Science, Vol. 2137. Springer, 13–26.

[22] X. Song, F. Liu, C. Yang, X. Luo, and Y. Zhang. 2015. Steganalysis of Adaptive JPEG Steganography Using 2D Gabor Filters. In *Proceedings of the 3rd ACM Workshop on Information Hiding and Multimedia Security (IH&MMSec '15)*. 15–23.

[23] X. Xu, J. Dong, W. Wang, and T. Tan. 2015. Robust Steganalysis based on Training Set Construction and Ensemble Classifiers Weighting. In *2015 IEEE International Conference on Image Processing (ICIP)*. 1498–1502.